Eur. Phys. J. B **34**, 143–153 (2003)
DOI: 10.1140/epjb/e2003-00206-4

THE EUROPEAN PHYSICAL JOURNAL B

# Photoconductivity detected magnetic resonance (PDMR) in crystalline tetracene

T. Barhoumi[1,a], S. Romdhane[2], A. Ben Fredj[1], F. Henia[3], and H. Bouchriha[1]

[1] Faculté des Sciences de Tunis, Laboratoire de Physique de la Matière Condensée, Campus universitaire, Tunis 1002, Tunisia
[2] Département de physique, Faculté des Sciences de Bizerte, 7021 Jarzouna, Bizerte, Tunisia
[3] École Supérieure des Sciences et Techniques de Tunis, Tunisia

Received 17 September 2002 / Received in final form 6 March 2003
Published online 4 August 2003 – 

**Abstract.** A detailed experimental study of the modulation by a high power microwave of induced exciton photoconductivity in crystalline tetracene is presented. These experiments, so called PDMR (Photoconductivity Detected Magnetic Resonance) are supported by a theoretical model based on a matrix density formalism and taking into account the fission of singlet excitons, dimensionality of triplet excitons motions and singlet and triplet detrapping of charge carriers. The best agreement between the observed PDMR lines and calculated curves allows the determination of the pertinent parameters governing the different process involved in the description of the photoconductivity mechanism.

**PACS.** 72.20.Jv Charge carriers: generation, recombination, lifetime, and trapping – 71.35.Aa Frenkel excitons and self-trapped excitons – 76.70. Hb Optically detected magnetic resonance (ODMR)

## 1 Introduction

Excited in its singlet absorption band crystalline tetracene becomes very photoconductive when it is submitted to an injecting contact [1]. This photoconductivity has already been the subject of many studies [2–4] but the situation is still confused with regard to the mechanisms which govern it. The photocurrent thus generated has indeed various origins which are principally the detrapping of trapped carriers by singlet excitons created directly by the exciting light and the detrapping of these carriers by triplet excitons created by the fission of singlets; this fission, energetically possible in the tetracene, [5] constitutes the principal channel of singlet decay. The evidence of these detrapping processes was confirmed by the modulation of photoconductivity by a static magnetic field [2,6,7], but the evaluation of the various contributions is unknown because of the absence of clean experimental results and complete theoretical models. Furthermore, if the modulation of fission by a magnetic field was observed [8–10] and well interpreted within the kinetic model of Johnson-Merrifield [11] and the kinematics model of Suna [12], it's not the same for the study of the triplet-triplet and triplet-doublet interactions and because the triplet absorption is only observed in the infra-red [13] what makes the direct creation of the triplets by conventional sources difficult.

In this work we present an experimental study of the photoconductivity modulation by microwave power in crystalline tetracene and an interpretation of the results within the framework of the kinematics model in order to highlight the contributions of the triplet-triplet and triplet-doublet interactions in the PDMR signal.


(a) (b)

**Fig. 1.** Samples: a) Electrodes placed on the same face of the crystal. b) Electrodes placed on both sides of the crystal.

## 2 Experimental study

### 2.1 Experimental device

Experiments are performed on tetracene crystals 50 to 100 $\mu$m thick grown by sublimation on the $a'b$ plane with a surface of about 0,5 cm$^2$. We have used two types of samples:

– a samples where we have deposited at the edges of the upper face two contacts of silver lacquer, supporting two thin copper wires to transmit the electric excitations (Fig. 1a).

– a samples where we have evaporated on the upper face a semi transparent gold layer and on the other face

[a] e-mail: tarek.barhoumi@webmails.com

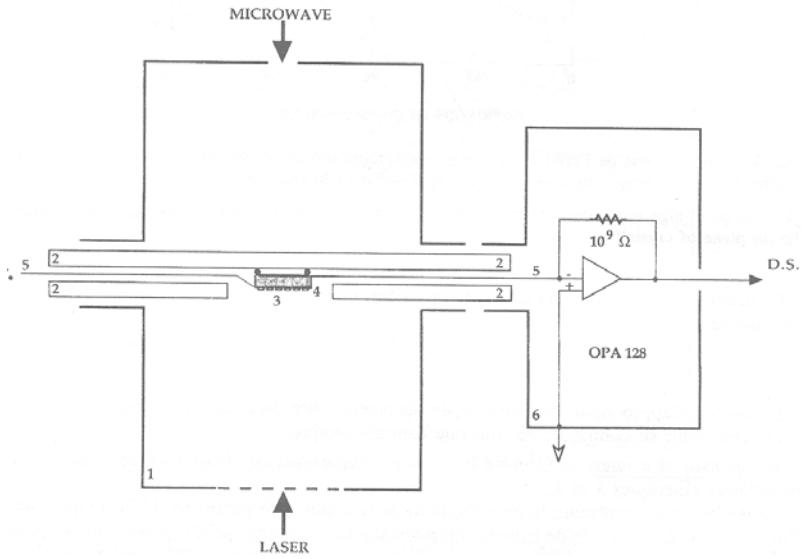


**Fig. 2.** Position of the sample in the cavity and schematic of the amplifier.

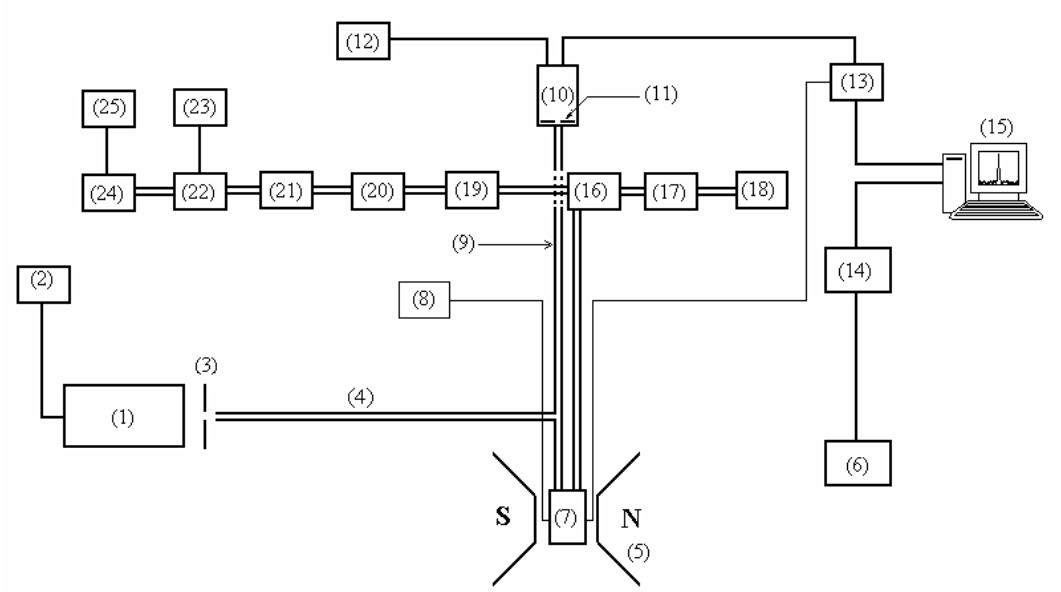


**Fig. 3.** Experimental setup.

an aluminum layer of the same surface. Two copper wires fixed with lacquer of silver ensure the contacts (Fig. 1b).

The crystal is placed on the central part of a Teflon cylinder 8 mm in diameter (Fig. 2) and presenting two axial traverses allowing the passage of the conducting wire. This axial electric geometry avoids in principle the perturbation of the magnetic field lines by the metallic conductors.

The Teflon cylinder is then introduced into the central axis of a rectangular cavity ($Varian\ TE_{102}$) on a side coupled by an iris with the wave guide and on the other side closed by a grid which allows the illumination of the sample by a laser beam.

One is connected to a stabilized power supply. The other wire carrying away the electrical current generated by the sample and which has a low intensity ($10^{-10}$ to $10^{-8}$ A), is linked to the entry of a low noise amplifier having an impedance of 1 Giga ohm and is immediately placed after the Teflon cylinder. The output of the amplifier voltage from 10 mV to 10 V goes to the input of a lockin analyser ($Model\ SRS830\ DSP$) having as a reference the magnetic field or the microwave power modulation frequency.

A microwave frequency of 9.4 GHz coming from a Gun diode and modulated in power by a PIN diode ($FMI\ Model\ 16/12$) in square signals of 1 kHz is transmitted to a backward wave oscillator (*top varian*) delivering a power of 6 W. The microwave thus amplified arrives in the cavity resonator by means of a wave guide and a circulator. A detector makes it possible to check the adaptation of the cavity (Fig. 3).

The cavity is placed in the gap of an electromagnet which can turn in the horizontal plane with an angle of 0.5°. This electromagnet supply is controlled by a Pentium II computer.

The output of the lockin analyser is digitalized by an input/output chart of the microcomputer.

### 2.2 Experimental results

On account of the adopted geometry, the measured currents are weak and relatively noisy. To improve the quality of the signal one made several accumulations (generally more than 8) to have an exploitable spectrum.

The Photocurrent obtained by exciting the crystal in its singlet absorption band by the ray 4880 Å of an argon laser (*Spectra physics* 165), is at least of an order of magnitude higher than the dark current.

We have used several crystals and recorded many PDMR spectra representing the relative variation of the photocurrent according to the magnetic field intensity under strong microwave power. All these spectra, although often noisy, present only one line centered on the field $H_0 \approx 3390$ G.

In view of the rectangular shape of the cavity and the obstruction of the gap of the electromagnet, it was difficult for us to modify the orientation of the magnetic field in the $a'b$ plan of the crystal and thus to obtain for the same sample PDMR spectra covering all the orientations. However, we have performed two different directions of the magnetic field corresponding respectively to the angles $\varphi = 20°$ and $\varphi = 50°$ from the crystalline axis $\vec{a}$.

Figure 4a shows a PDMR spectrum recorded for a direction of the magnetic field forming an angle $\varphi = 20°$ from the crystalline axis $\vec{a}$. For this direction one notices that the maximum effect measured is about 0.12% and corresponds to an increase in photoconductivity. The PDMR line full-width at half maximum is about 60 gauss.

On Figure 4b we have presented a spectrum corresponding to the direction $\varphi = 50°$ near to the direction of the resonance of the static effect [14]. On this spectrum we can distinguish a well resolved central line of which the effect is about 0.13%.

We notice that, in the case of tetracene, and for the orientations used, the PDMR spectra present only one line centered on the field $H_0$. This situation is different from that observed in crystalline anthracene [15,16] where the PDMR spectra present three lines, one centered on the field $H_0$ and two lines located on both sides of this central field.

One can attribute the single line to the presence of a trap but this supposition cannot be possible because this line is centred in the triplet band ($h\upsilon = 0.3$ cm$^{-1}$) and is always reproduced in the same position and moreover its intensity is of the same order of magnitude as that of PDMR lines observed in anthracene [16].

The modulation observed in tetracene seems therefore to be the result of various mechanisms which we will try to evaluate in this work.

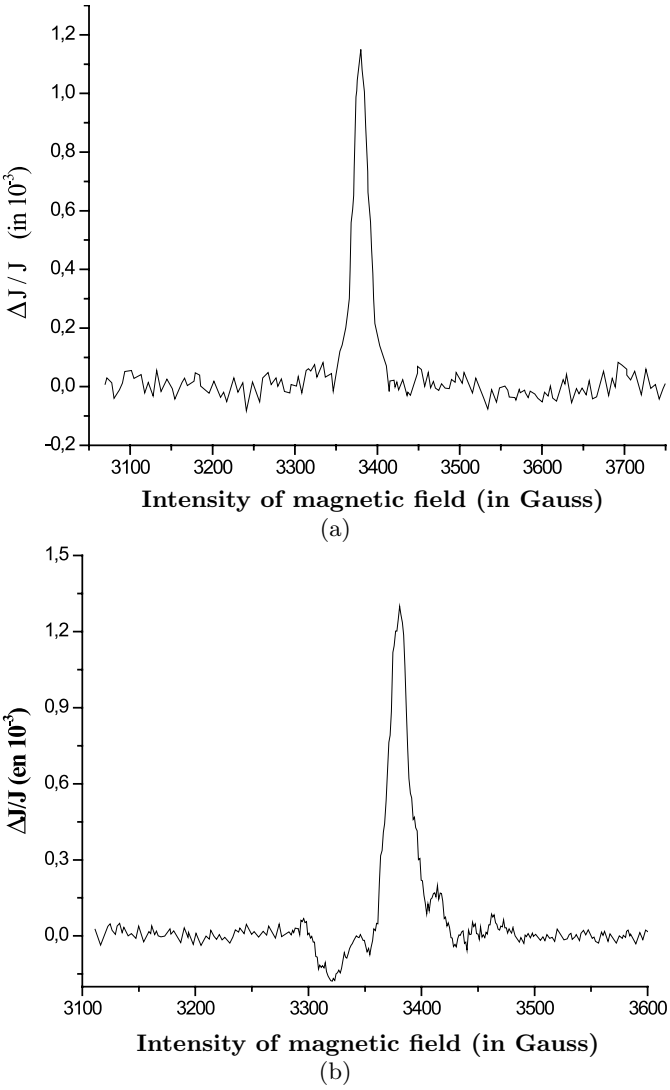


**Fig. 4.** (a) PDMR Spectrum on a crystal of tetracene. (b) PDMR Spectrum on a second crystal of tetracene.

## 3 Origin of the modulation of the photoconductivity

When a crystal of tetracene was excited in its singlet absorption band where we have beforehand injected holes, one observes a photocurrent $J$ much higher than the dark current $J_0$ ($J/J_0 \simeq 100$). This photocurrent comes mainly from the detrapping in the volume of trapped carriers by singlet excitons and by triplet excitons created by the fission of the singlets. One can consider a self-ionization of excitons on the surface but the illumination being weak [2], this contribution is negligible, on the other hand it is probable that a detrapping by the photons is active. By taking into account these various mechanisms, the densities of the free charges $N_f$ can be described by the equation:

$$\frac{\mathrm{d}N_f}{\mathrm{d}t} = \eta_s R_s N_t n_s + \eta_T R_T N_t n_T + \sigma \Phi N_t - \frac{N_f}{\tau_t}, \quad (1)$$

where $\eta_s$ and $\eta_T$ are the yield of detrapping holes trapped by the singlet and the triplet excitons, $R_s$ and $R_T$ are respectively the rate constants of singlet-trapped carrier and triplet-trapped carrier interactions, $N_t$ the density of trapped carriers, $n_s$ and $n_T$ the densities of singlet and triplet excitons, $\sigma$ the cross-section for hole photodetrapping, $\Phi$ the number of incident photons per $\mathrm{cm}^2\,\mathrm{s}^{-1}$ and $\tau_t$ the trapping time of the free charges.

At equilibrium we obtain:

$$N_f = \tau_t N_t \left(\eta_s R_s n_s + \eta_T R_T n_T + \sigma\Phi\right), \tag{2}$$

and the detrapping photocurrent is:

$$J = \mu N_f e E, \tag{3}$$

$\mu$ being the carriers training mobility, $e$ the electron charge, and $E$ the average electric field in the crystal.

The singlet-carrier interaction rate constant $R_s$ is independent of the magnetic field [17]. The observed effect is therefore due to the modulation by this field of the triplet-doublet interaction rate constant $R_T$ and of the densities of triplet ($n_T$) and singlet ($n_s$) excitons.

The modulation of $R_T$ by the magnetic field is already well known [18,19], it is the same for $n_s$ and possibly for $n_T$.

Furthermore for the used illumination intensities $\Phi \approx 10^{13} - 10^{14}$ photons/$\mathrm{cm}^2$ the detrapping by the photons is negligible $\left(\sigma \approx 10^{-18}\ \mathrm{cm}^2\right)$ [20] compared to the other generation processes of the carriers so that one will have:

$$N_f = \tau_t N_t \left(\eta_s R_s n_s + \eta_T R_T n_T\right), \tag{4}$$

$$= \tau_t N_t \left(R_s^{'} n_s + R_T^{'} n_T\right), \tag{5}$$

where we have posed $R_s^{'} = \eta_s R_s$ and $R_T^{'} = \eta_T R_T$.

To get $n_s$ and $n_T$ it is enough to write their kinetics evolution when the crystal is excited by an uniform illumination in its singlet absorption band. One has in this case:

$$\frac{\mathrm{d}n_s}{\mathrm{d}t} = \alpha_s\Phi - k_s n_s + \frac{1}{2}\gamma_s n_T^2, \tag{6}$$

$$\frac{\mathrm{d}n_T}{\mathrm{d}t} = \left(2k_f + k_{CI}\right) n_s - \beta_0 n_T - \gamma_{sT} n_s n_T - \gamma n_T^2, \tag{7}$$

where $\alpha_s$ is the singlet absorption coefficient, $k_s$ is the total desactivation rate constant of the singlet, it includes at the same time the channels of radiative desactivation ($k_r$) and of radiationless desactivation (inter-system crossing $k_{CI}$ and fission $k_f$):

$$k_s = k_r + k_{CI} + k_f, \tag{8}$$

$\gamma_s$ is the rate constant of triplet fusion to give an excited singlet, $\beta_0^{-1}$ is the triplet lifetime, $\gamma$ is the triplet-triplet rate constant interaction, $\gamma_{sT}$ is the singlet-triplet rate constant interaction.

In the case of weak illumination $\gamma_s n_T^2$, $\gamma_{sT} n_s n_T$ and $\gamma n_T^2$ are negligible compared to the other terms [2]. Furthermore, fission is the most dominant channel of singlet desactivation in crystalline tetracene ($k_s \approx k_f$) [7,8,21] so one will have:

$$\frac{\mathrm{d}n_s}{\mathrm{d}t} \approx \alpha_s\Phi - k_s n_s, \tag{9}$$

$$\frac{\mathrm{d}n_T}{\mathrm{d}t} \approx 2k_s n_s - \beta_0 n_T, \tag{10}$$

which at equilibrium leads to:

$$n_s = \frac{\alpha_s\Phi}{k_s}, \tag{11}$$

$$n_T = \frac{2k_s n_s}{\beta_0}. \tag{12}$$

The triplet and the singlet densities will thus depend on the magnetic field, through $k_s$:

$$\frac{\Delta n_s}{n_s} = -\frac{\Delta k_s}{k_s}, \tag{13}$$

$$\frac{\Delta n_T}{n_T} = \frac{\Delta k_s}{k_s}, \tag{14}$$

and as $k_s \approx k_f = \gamma_s^{'} n_{s0}$ [21,22] where $\gamma_s^{'}$ is the rate constant of fission and $n_{s0}$ the density of molecules in the ground state $S_0$ one has:

$$\frac{\Delta k_s}{k_s} = \frac{\Delta\gamma_s^{'}}{\gamma_s^{'}}. \tag{15}$$

That is to say:

$$\frac{\Delta n_s}{n_s} = -\frac{\Delta\gamma_s^{'}}{\gamma_s^{'}}, \tag{16}$$

$$\frac{\Delta n_T}{n_T} = \frac{\Delta\gamma_s^{'}}{\gamma_s^{'}}. \tag{17}$$

The effect observed on the photocurrent is thus due to the modulation by the magnetic field of the triplet-doublet rate constant interaction and the rate constant of fission $\left(\gamma_s^{'}\right)$.

We have:

$$\frac{\Delta J}{J} = \frac{\Delta N_f}{N_f}, \tag{18}$$

which is evaluated more simply by:

$$\Delta N_f = \tau_t N_t \left(R_s^{'}\Delta n_s + R_T^{'}\Delta n_T + n_T \Delta R_T^{'}\right), \tag{19}$$

$$\frac{\Delta N_f}{N_f} = \frac{R_s^{'}\Delta n_s + R_T^{'}\Delta n_T + n_T\Delta R_T^{'}}{R_s^{'} n_s + R_T^{'} n_T}. \tag{20}$$

While replacing (16) and (17) in (20), the modulation of the total photocurrent is:

$$\frac{\Delta J}{J} = a\frac{\Delta\gamma_s^{'}}{\gamma_s^{'}} + b\frac{\Delta R_T}{R_T} \tag{21}$$

with:

$$a = \frac{R_T^{'} n_T - R_s^{'} n_s}{R_s^{'} n_s + R_T^{'} n_T}, \tag{22}$$

$$b = \frac{R_T^{'} n_T}{R_s^{'} n_s + R_T^{'} n_T}, \tag{23}$$

while posing:

$$\delta = \frac{R_s^{'} n_s}{R_T^{'} n_T}, \tag{24}$$

where $\delta$ is the rate constant of the detrapping by the singlet and the triplet excitons.

Thus, we can write:

$$a = \frac{1-\delta}{1+\delta}, \tag{25}$$

$$b = \frac{1}{1+\delta}. \tag{26}$$

According to [2] one can write that $R_s^{'} n_s < R_T^{'} n_T$ which gives $\delta < 1$.

Thus the modulation of the total observed photocurrent appears as the weighted sum respectively of the modulation of fluorescence ($\frac{\Delta\gamma_s^{'}}{\gamma_s^{'}}$) and the detrapping photocurrent ($\frac{\Delta R_T}{R_T}$). It is thus possible to evaluate the contribution of each process from the spectra modulation by a microwave of the total photocurrent (PDMR) and the fluorescence (ODMR).

## 4 Theoretical study

### 4.1 Microwave effect at high field on the photoconductivity

#### 4.1.1 Interaction Hamiltonian

The Triplet Doublet (T-D) interaction will be described by an interaction Hamiltonian $\mathcal{H}_0$ of the form:

$$\mathcal{H}_0 = \mathcal{H}_{ss} + g_T \mu_B \overrightarrow{H}\ \overrightarrow{S}_T + g_D \mu_B \overrightarrow{H}\ \overrightarrow{S}_D, \tag{27}$$

where $\mathcal{H}_{ss}$ is the spin Hamiltonian of the triplet exciton, $\overrightarrow{S}_T$ and $\overrightarrow{S}_D$ are respectively the triplet and the doublet spin operators, $\overrightarrow{H}$ is the magnetic field, $\mu_B$ the Bohr magneton, $g_T$ and $g_D$ the Lande factors of the triplet and the doublet where one takes $g_T = 2,0032$ and $g_D = 2,0023$ [15].

The diagonalization of this Hamiltonian in the basis $\left\{\left|X \pm \frac{1}{2}\right\rangle, \left|Y \pm \frac{1}{2}\right\rangle, \left|Z \pm \frac{1}{2}\right\rangle\right\}$; the tensorial product of the basis $\{|X\rangle, |Y\rangle, |Z\rangle\}$ of the triplet and the basis $\left\{\left|\pm\frac{1}{2}\right\rangle\right\}$ formed by the eigenstates of the doublet, gives us the six eigenstates of the (T-D) pair and their corresponding eigenvalues (Tab. 1).

The doublet character [19] of the six states of the pair is obtained by projecting these states on a pure doublet state $|D\rangle$ verifying:

$$S^2 |D\rangle = (S_T + S_D)^2 |D\rangle = \frac{3}{4} |D\rangle. \tag{28}$$

**Table 1.** Eigenstates and eigenvalues of T-D pair.

| **Eigenstates** | **Eigenvalues** |
|---|---|
| $\left\|1, \frac{1}{2}\right\rangle \equiv \|1\rangle$ | $\varepsilon_1 = \left(g_T + \frac{1}{2} g_D\right) \mu_B H - \frac{\varepsilon_0}{2}$ |
| $\left\|1, -\frac{1}{2}\right\rangle \equiv \|2\rangle$ | $\varepsilon_2 = \left(g_T - \frac{1}{2} g_D\right) \mu_B H - \frac{\varepsilon_0}{2}$ |
| $\left\|0, \frac{1}{2}\right\rangle \equiv \|3\rangle$ | $\varepsilon_3 = \frac{1}{2} g_D \mu_B H + \varepsilon_0$ |
| $\left\|0, -\frac{1}{2}\right\rangle \equiv \|4\rangle$ | $\varepsilon_4 = -\frac{1}{2} g_D \mu_B H + \varepsilon_0$ |
| $\left\|-1, \frac{1}{2}\right\rangle \equiv \|5\rangle$ | $\varepsilon_5 = \left(-g_T + \frac{1}{2} g_D\right) \mu_B H - \frac{\varepsilon_0}{2}$ |
| $\left\|-1, \frac{1}{2}\right\rangle \equiv \|6\rangle$ | $\varepsilon_6 = \left(-g_T - \frac{1}{2} g_D\right) \mu_B H - \frac{\varepsilon_0}{2}$ |

$$\varepsilon_0 = D^* \left(\frac{1}{3} - n^2\right) + E^* \left(m^2 - l^2\right)$$

At zero field this state is:

$$|D_\pm\rangle = \frac{1}{\sqrt{3}} \left[\left|X \pm \frac{1}{2}\right\rangle + i \left|Y \pm \frac{1}{2}\right\rangle - \left|Z \mp \frac{1}{2}\right\rangle\right]. \tag{29}$$

At zero field the doublet character is uniformly distributed over the six states of the pair with a weight $\frac{1}{3}$.

#### 4.1.2 Microwave Hamiltonian

The Hamiltonian associated with the radio-frequency field applied perpendicular to the static field $H_0$ is written:

$$\mathcal{H}_1 = g \mu_B H_1 S_X \cos(\omega t), \tag{30}$$

where $S_X$ is the projection of the spin operator $\vec{S}$ on $X$ axis of the zero-field structure, $H_1$ is the radio-frequency field intensity and $\omega$ its pulsation.

#### 4.1.3 Transitions microwaves

The possible transitions between the (T-D) pair states $|i\rangle$ and $|j\rangle$ are: $\Delta m = \pm 1$ and $\Delta S = 0$ with the probability:

$$P_{ij} = |\langle i| S_X |j\rangle|^2. \tag{31}$$

It would be necessary to evaluate the matrix elements $S_X$ in a basis of spin states which diagonalize the spin Hamiltonian of the T-D pair.

The matrix elements $S_X$ are written [15]:

$$S_X = \begin{pmatrix} 0 & \frac{1}{2} & \frac{1}{\sqrt{2}} & 0 & 0 & 0 \\ \frac{1}{2} & 0 & 0 & \frac{1}{\sqrt{2}} & 0 & 0 \\ \frac{1}{\sqrt{2}} & 0 & 0 & \frac{1}{2} & \frac{1}{\sqrt{2}} & 0 \\ 0 & \frac{1}{\sqrt{2}} & \frac{1}{2} & 0 & 0 & \frac{1}{\sqrt{2}} \\ 0 & 0 & \frac{1}{\sqrt{2}} & 0 & 0 & \frac{1}{2} \\ 0 & 0 & 0 & \frac{1}{\sqrt{2}} & \frac{1}{2} & 0 \end{pmatrix}. \tag{32}$$

The possible transitions are determined by $P_{ij} \neq 0$.

**Table 2.** Probabilities and energies of the microwave transitions.

| Transitions | Probabilities | Energies |
|---|---|---|
| $\|1\rangle \Longleftrightarrow \|2\rangle$ | $\frac{1}{4}$ | $\varepsilon_1 - \varepsilon_2 = g_D \mu_B H$ |
| $\|1\rangle \Longleftrightarrow \|3\rangle$ | $\frac{1}{2}$ | $\varepsilon_1 - \varepsilon_3 = g_T \mu_B H - \frac{3}{2}\varepsilon_0$ |
| $\|2\rangle \Longleftrightarrow \|4\rangle$ | $\frac{1}{2}$ | $\varepsilon_2 - \varepsilon_4 = g_T \mu_B H - \frac{3}{2}\varepsilon_0$ |
| $\|3\rangle \Longleftrightarrow \|4\rangle$ | $\frac{1}{4}$ | $\varepsilon_3 - \varepsilon_4 = g_D \mu_B H$ |
| $\|3\rangle \Longleftrightarrow \|5\rangle$ | $\frac{1}{2}$ | $\varepsilon_3 - \varepsilon_5 = g_T \mu_B H + \frac{3}{2}\varepsilon_0$ |
| $\|4\rangle \Longleftrightarrow \|6\rangle$ | $\frac{1}{2}$ | $\varepsilon_4 - \varepsilon_6 = g_T \mu_B H + \frac{3}{2}\varepsilon_0$ |
| $\|5\rangle \Longleftrightarrow \|6\rangle$ | $\frac{1}{4}$ | $\varepsilon_5 - \varepsilon_6 = g_D \mu_B H$ |

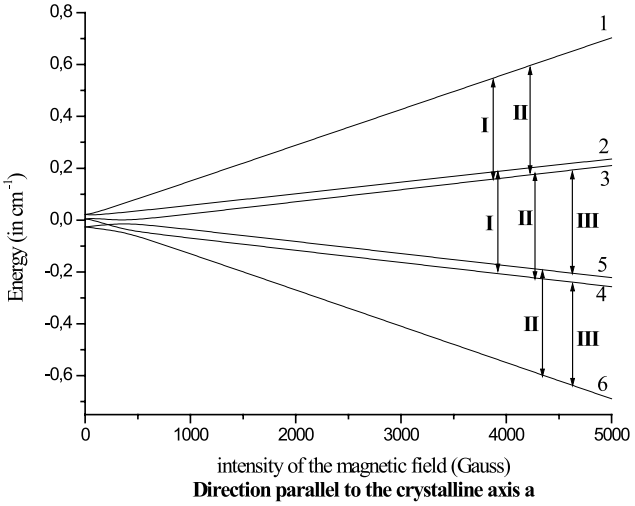


**Fig. 5.** The scheme of Zeeman sublevels of a doublet-triplet exciton pair in a strong magnetic field. The vertical arrows show the resonance transitions accompanying the absorption of the microwave power. Six magnetic sublevels containing quintuplet and singlet spin configurations are shown.

In Table 2 we give the possible transitions as well as the corresponding energies and probabilities.

In Figure 5 we have represented the evolution of the (T-D) pair energies in crystalline tetracene according to the intensity of the static magnetic field and parallel to the direction of the crystalline axis $\vec{a}$. The vertical arrows represent the possible induced transitions by the microwaves.

There are three energies of transition, the PDMR spectrum corresponding to the triplet-doublet interaction would thus have three constituant lines of which one is centered on a field $H_0$ and two others are located on either sides of the field $H_0$.

## 4.2 Kinematics theory of PDMR effect

### 4.2.1 Model

To describe the evolution of the pair we follow a similar step to that introduced by Suna [12] for the description of the triplet-triplet interaction. We have used a matrix density formalism in which the motion of the exciton is described in the approximation of the hopping model [12].

The pair-density-matrix evolution equation is written in the form:

$$\begin{aligned}\frac{\mathrm{d}\rho}{\mathrm{d}t} = &-\frac{\mathrm{i}}{\hbar}\left[\mathcal{H}, \rho\left(\overrightarrow{R}\right)\right] - 2\beta\rho\left(\overrightarrow{R}\right) \\ &+2\sum_{\overrightarrow{R}'}\psi\left(\overrightarrow{R}'\right)\left[\rho\left(\overrightarrow{R}+\overrightarrow{R}'\right) - \rho\left(\overrightarrow{R}\right)\right] \\ &-\delta\left(\overrightarrow{R}\right)\frac{\lambda}{2}\left[\sigma, \rho\left(\overrightarrow{0}\right)\right]^{+} + S(\overrightarrow{R}),\end{aligned} \tag{33}$$

where $[..,..]$ stands for the commutator and $[...,...]^{+}$ for the anticommutator, $\rho\left(\overrightarrow{R}\right)$ being the density matrix for a pair separated by a distance $\overrightarrow{R}$, $\mathcal{H} = \mathcal{H}_0 + \mathcal{H}_1$ in which $\mathcal{H}_0$ is the static-field spin Hamiltonian and $\mathcal{H}_1$ is the perturbation by the microwave field of strength $H_1$ and frequency $\omega$ [22,23]. The quantity $\beta$ in the second term of the right-hand side is the effective single-exciton decay rate [12,24] in the dimension of motion having an isotropic diffusion constant $D$ [24,25]. In the third term, the quantities $\psi\left(\overrightarrow{R}'\right)$ are the hopping rates between sites separated by distances $R^{'}$, the sum being taken over all sites. The rate $\lambda$ is the nearest-neighbor pair-interaction rate leading to the doublet, and $\sigma = [|D_+\rangle\langle D_+| + |D_-\rangle\langle D_-|]$ [15] is the doublet-state projection matrix. Finally, $S(\overrightarrow{R})$ is the pair-source term which is of the form [19]:

$$S(\overrightarrow{R}) = \alpha I, \tag{34}$$

in which $I$ is the unit matrix and $\alpha = \frac{nN}{6}\beta v^2$ where $n$ and $N$ are respectively the unpaired-triplet-exciton and the doublet densities in the crystal [24]. $v$ is, according to the dimensionality of the movement of the exciton, a volume, a surface or a length corresponding to the area of the crystal where the movement is localised.

The solution of (33) can be written in the form [22,23]:

$$\rho\left(\overrightarrow{R}\right) = \rho^{00}\left(\overrightarrow{R}\right) + Z(R)\mathrm{e}^{-\mathrm{i}\omega t} + \overline{Z}(R)\mathrm{e}^{\mathrm{i}\omega t} + \rho^{02}\left(\overrightarrow{R}\right)H_1^2, \tag{35}$$

where one has three unknown matrices, namely, $\rho^{00}\left(\overrightarrow{R}\right)$ for the usual static field, an auxiliary matrix $Z(\overrightarrow{R})$, which allows one to get the matrix $\rho^{02}\left(\overrightarrow{R}\right)$.

The resolution of equation (33) in dynamic mode $\left(\frac{\mathrm{d}\rho\left(\overrightarrow{R}\right)}{\mathrm{d}t} \neq 0\right)$ enables us to determine the matrix elements $\rho^{00}\left(\overrightarrow{R}\right)$, $\rho^{02}\left(\overrightarrow{R}\right)$ and to deduce the evolution of the photoconductivity under the effect of the microwave power via the relation [26]:

$$\frac{\Delta R}{R} = \frac{\mathrm{Tr}\left(\sigma\rho^{02}\left(\overrightarrow{R}\right)\right)}{\mathrm{Tr}\left(\sigma\rho^{00}\left(\overrightarrow{R}\right)\right)}. \tag{36}$$

Substituting (35) in (33), one gets the system of three matrix equations:

$$0 = -\frac{\mathrm{i}}{\hbar}\left[\mathcal{H}_0, \rho^{00}\left(\overrightarrow{R}\right)\right] - 2\beta\rho^{00}\left(\overrightarrow{R}\right) + 2\sum_{\overrightarrow{R}'}\psi\left(\overrightarrow{R}'\right)\left[\rho^{00}\left(\overrightarrow{R}+\overrightarrow{R}'\right) - \rho^{00}\left(\overrightarrow{R}\right)\right] - \delta\left(\overrightarrow{R}\right)\frac{\lambda}{2}\left[\sigma, \rho^{00}\left(\overrightarrow{0}\right)\right]^{+} + S(\overrightarrow{R}), \quad (37)$$

$$-\mathrm{i}\omega Z(\overrightarrow{R}) = -\frac{\mathrm{i}}{\hbar}\left[\mathcal{H}_0, Z\left(\overrightarrow{R}\right)\right] - 2\beta Z\left(\overrightarrow{R}\right) + 2\sum_{\overrightarrow{R}'}\psi\left(\overrightarrow{R}'\right)\left[Z\left(\overrightarrow{R}+\overrightarrow{R}'\right) - Z\left(\overrightarrow{R}\right)\right] - \delta\left(\overrightarrow{R}\right)\frac{\lambda}{2}\left[\sigma, Z\left(\overrightarrow{0}\right)\right]^{+} - \frac{\mathrm{i}}{2\hbar}\left[\rho^{00}\left(\overrightarrow{R}\right), \mathcal{H}_1\right], \quad (38)$$

$$0 = -\frac{\mathrm{i}}{\hbar}\left[\mathcal{H}_0, \rho^{02}\left(\overrightarrow{R}\right)\right] - 2\beta\rho^{02}\left(\overrightarrow{R}\right) + 2\sum_{\overrightarrow{R}'}\psi\left(\overrightarrow{R}'\right)\left[\rho^{02}\left(\overrightarrow{R}+\overrightarrow{R}'\right) - \rho^{02}\left(\overrightarrow{R}\right)\right] - \delta\left(\overrightarrow{R}\right)\frac{\lambda}{2}\left[\sigma, \rho^{02}\left(\overrightarrow{0}\right)\right]^{+} - \frac{\mathrm{i}}{2\hbar}\left[Z\left(\overrightarrow{R}\right), \mathcal{H}_1\right]. \quad (39)$$

Let us express (37, 38) and (39) in a basis of spin state $\{|m\rangle\}$ which diagonalizes the static-field spin Hamiltonian $\mathcal{H}_0$ with eigenvalues $E_m$, then

$$\mathcal{H}_0\,|m\rangle = E_m\,|m\rangle\,. \quad (40)$$

This choice of basis uncouples the equations for the various matrix elements of $\rho^{00}\left(\overrightarrow{R}\right)$, $Z\left(\overrightarrow{R}\right)$ and $\rho^{02}\left(\overrightarrow{R}\right)$, and leads us to use the Green's functions $G\left(\beta, \overrightarrow{R}\right)$, satisfying the hopping diffusion equation

$$\sum_{\overrightarrow{R}'}\psi\left(\overrightarrow{R}'\right)\left[G\left(\beta, \overrightarrow{R}+\overrightarrow{R}'\right) - G\left(\beta, \overrightarrow{R}\right)\right] - \beta G\left(\beta, \overrightarrow{R}\right) = \delta_{\overrightarrow{R},\overrightarrow{0}}, \quad (41)$$

where $\delta_{\overrightarrow{R},\overrightarrow{0}}$ is the $\delta$ function $\delta_{\overrightarrow{0},\overrightarrow{0}} = 1$, $\delta_{\overrightarrow{R},\overrightarrow{0}} = 0$ for $\overrightarrow{R} \neq \overrightarrow{0}$ (Eqs. (35) and (38) of Ref. [12]).

By introducing the following notations:

$$\omega_{mn} = (E_m - E_n)/\hbar,\ \Omega_{mn} = \omega_{mn} - \omega,$$
$$\beta_{mn} = \beta + \mathrm{i}\omega_{mn}/2,\ \widetilde{\beta}_{mn} = \beta + \mathrm{i}\Omega_{mn}/2,$$
$$G\left(\beta_{mn}, \overrightarrow{0}\right) = G\left(\beta_{mn}\right), \quad (42)$$

one can get the formal solution of (37, 38) and (39) in the smooth approximation [12] of the form:

$$\rho^{00}(R) = \frac{\alpha}{2\beta}\delta_{mn} + \frac{\lambda}{4}G\left(\beta_{mn}, R\right)\left[\sigma, \rho^{00}(0)\right]^{+}_{mn}, \quad (43)$$

$$Z_{mn}(R) = \frac{\lambda}{4}G\left(\widetilde{\beta}_{mn}, R\right)[\sigma, Z(0)]^{+}_{mn} + \frac{\mathrm{i}}{2\hbar H_1^2}\sum_{R'}G\left(\widetilde{\beta}_{mn}, R-R'\right)\left[\rho^{00}\left(R'\right), \mathcal{H}_1\right]_{mn}, \quad (44)$$

$$\rho^{02}(R) = \frac{\lambda}{4}G\left(\beta_{mn}, R\right)\left[\sigma, \rho^{02}(0)\right]^{+}_{mn} + \frac{\mathrm{i}}{2\hbar H_1^2} \times \sum_{R'}G\left(\beta_{mn}, R-R'\right)\left[Z\left(R'\right) + \overline{Z}\left(R'\right), \mathcal{H}_1\right]_{mn}. \quad (45)$$

### 4.2.2 High field kinematics model

By high field, it is meant here any field strength in which the Zeeman energy is much larger (say, by one order of magnitude) than the zero field splitting (ZFS) energies. In the present case, experiments were performed at 5 kG. In a high field the only possible transitions are:

$$\Omega_{-1} = \Omega_{24} = \Omega_{13},$$
$$\Omega_0 = \Omega_{12} = \Omega_{34} = \Omega_{56},$$
$$\Omega_1 = \Omega_{35} = \Omega_{46}. \quad (46)$$

The doublet character is distributed as follows:

$$\sigma_{11} = \sigma_{11} = 0,$$
$$\sigma_{22} = \sigma_{55} = \frac{2}{3},$$
$$\sigma_{33} = \sigma_{44} = \frac{1}{3}. \quad (47)$$

Referring to (36) the relative photoconductivity variation is then written:

$$\frac{1}{H_1^2}\left(\frac{\Delta R}{R}\right) = \frac{\sigma_{22}\left(\rho_{22}^{02}(R) + \rho_{55}^{02}(R)\right) + \sigma_{33}\left(\rho_{33}^{02}(R) + \rho_{44}^{02}(R)\right)}{\sigma_{22}\left(\rho_{22}^{00}(R) + \rho_{55}^{00}(R)\right) + \sigma_{33}\left(\rho_{33}^{00}(R) + \rho_{44}^{00}(R)\right)}. \quad (48)$$

The only terms to be calculated will be thus: $\rho_{ii}^{02}(R)$ and $\rho_{ii}^{00}(R)$ with $i = 2, 3, 4, 5$.

Equation (43), solved initially for $R = 0$, gives:

$$\rho_{mn}^{02}(R) = \frac{\alpha}{2\beta}\left(1 - G_r\frac{A_n - 1}{A_n}\right),\ \ 1 \leq n \leq 6. \quad (49)$$

The notation was simplified by introducing the definitions:

$$k = -\lambda G(\beta),\ \gamma = \frac{g\mu_B}{\hbar},\ G_r = \frac{G(\beta, R)}{G(\beta)}, A_3 = A_4 = 1 + \frac{k}{3},$$
$$A_2 = A_5 = 1 + \frac{2k}{3},\ A_1 = A_6 = 0. \quad (50)$$

If $H_0 = \omega/g_D\mu_B$ is the central field corresponding to the microwave frequency, one will have respectively the lower and the higher-field resonances occurring when:

$$\hbar\Omega_{13} = \hbar\Omega_{24} = g_T\mu_B H - \frac{3}{2}\varepsilon_0 - \hbar\omega, \quad (51)$$

and

$$\hbar\Omega_{35} = \hbar\Omega_{46} = g_T\mu_B H + \frac{3}{2}\varepsilon_0 - \hbar\omega, \tag{52}$$

vanishing for field $H_l < H_0$ and $H_h > H_0$. The central resonance corresponding to field $H = H_0$ occurs when:

$$\hbar\Omega_{12} = \hbar\Omega_{34} = \hbar\Omega_{56} = g_D\mu_B H - \hbar\omega, \tag{53}$$

vanishes.

For the transitions (51, 52) and (53) one gets, from (44) and (45) with the aid of the following property of the Green's functions

$$\sum_{R'} G(\beta_1, R - R')\, G(\beta_2, R') = \frac{G(\beta_2, R) - G(\beta_2, R)}{(\beta_2 - \beta_1)}, \tag{54}$$

the following matrix elements:

$$\rho_{22}^{02}(R) = \gamma^2 \frac{\alpha}{2\beta}\frac{2k}{3}\left[\frac{1}{\left(1+\frac{2k}{3}\right)}F\left(\widetilde{\beta}_{12}, R\right) - \frac{1}{\left(1+\frac{k}{3}\right)\left(1+\frac{2k}{3}\right)}F\left(\widetilde{\beta}_{24}, R\right)\right], \tag{55}$$

$$\rho_{33}^{02}(R) = \gamma^2 \frac{\alpha}{2\beta}\frac{2k}{3}\left[-\frac{1}{\left(1+\frac{k}{3}\right)\left(1+\frac{2k}{3}\right)}F\left(\widetilde{\beta}_{35}, R\right) - \frac{1}{\left(1+\frac{k}{3}\right)}F\left(\widetilde{\beta}_{13}, R\right)\right], \tag{56}$$

$$\rho_{44}^{02}(R) = \gamma^2 \frac{\alpha}{2\beta}\frac{2k}{3}\left[-\frac{1}{\left(1+\frac{k}{3}\right)\left(1+\frac{2k}{3}\right)}F\left(\widetilde{\beta}_{24}, R\right) - \frac{1}{\left(1+\frac{k}{3}\right)}F\left(\widetilde{\beta}_{46}, R\right)\right], \tag{57}$$

$$\rho_{55}^{02}(R) = \gamma^2 \frac{\alpha}{2\beta}\frac{2k}{3}\left[-\frac{1}{\left(1+\frac{2k}{3}\right)}F\left(\widetilde{\beta}_{56}, R\right) - \frac{1}{\left(1+\frac{k}{3}\right)\left(1+\frac{2k}{3}\right)}F\left(\widetilde{\beta}_{35}, R\right)\right]. \tag{58}$$

The relative variation of photoconductivity under the effect of a microwave power is written as the sum of three terms corresponding to the three possible transitions:

$$\frac{\Delta R}{R} = \left.\frac{\Delta R}{R}\right|_{\Omega_{-1}} + \left.\frac{\Delta R}{R}\right|_{\Omega_0} + \left.\frac{\Delta R}{R}\right|_{\Omega_{+1}}, \tag{59}$$

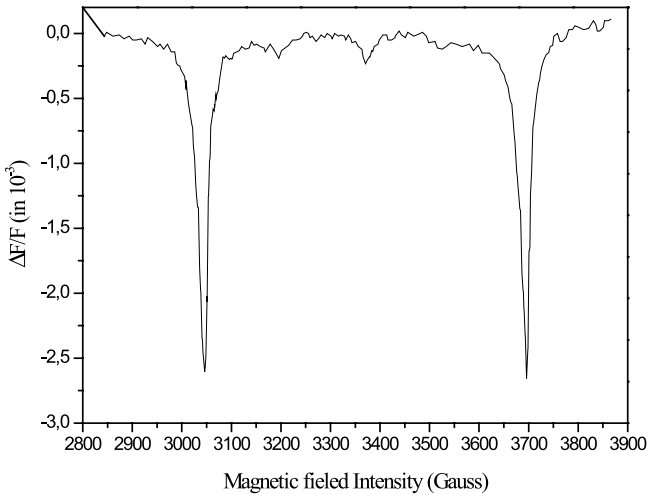


**Fig. 6.** ODMR spectrum for the direction $\varphi = 20°$.

with:

$$\left.\frac{\Delta R}{R}\right|_{\Omega_{-1}} = \frac{-\frac{k}{18}\gamma^2 H_1^2}{A_2A_3(1-G_r) + \left(1+\frac{4k}{9}\right)G_r} \times \left\{A_3\left[A_2(1-G_r)+G_r\right]F\left(\widetilde{\beta}_{24}, R\right) + A_2\left[A_3(1-G_r)+G_r\right]F\left(\widetilde{\beta}_{13}, R\right)\right\}, \tag{60}$$

$$\left.\frac{\Delta R}{R}\right|_{\Omega_0} = \frac{-\frac{k}{9}\gamma^2 H_1^2}{A_2A_3(1-G_r) + \left(1+\frac{4k}{9}\right)G_r} \times \left\{A_3\left[A_2(1-G_r)+G_r\right] \times \left[F\left(\widetilde{\beta}_{34}, R\right) + F\left(\widetilde{\beta}_{56}, R\right)\right]\right\}, \tag{61}$$

$$\left.\frac{\Delta R}{R}\right|_{\Omega_{+1}} = \frac{-\frac{k}{18}\gamma^2 H_1^2}{A_2A_3(1-G_r) + \left(1+\frac{4k}{9}\right)G_r} \times x\left\{A_3\left[A_2(1-G_r)+G_r\right]F\left(\widetilde{\beta}_{35}, R\right) + A_2\left[A_3(1-G_r)+G_r\right]F\left(\widetilde{\beta}_{46}, R\right)\right\}. \tag{62}$$

in which:

$$F\left(\widetilde{\beta}_{mn}, R\right) = \frac{1 - \mathrm{Re}\left[\frac{G(\widetilde{\beta}_{mn}, R)}{G(\beta)}\right]}{\Omega_{mn}^2}. \tag{63}$$

## 5 Kinematics interpretation of PDMR effect

For a correct interpretation of the experimental results on the photocurrent we have realized under the same conditions the ODMR experiments on the same crystal of tetracene.

In Figure 6 we have presented an ODMR spectrum for the direction $\varphi = 20°$. In reference [26] we have represented all the experimental results. The resonance spectra

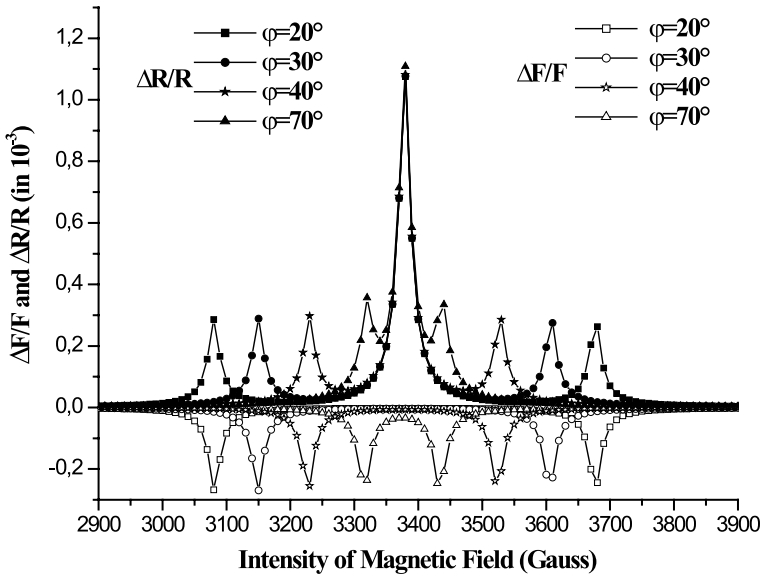


**Fig. 7.** Digital simulation of the modulation by a microwave power of the triplet-triplet interaction rate constant and the triplet-doublet interaction rate constant for various orientations of the magnetic field in the ab plane of crystalline tetracene.

**Table 3.** Kinematics parameters which gave the best fit.

| $D^*$ | $E^*$ | $R$ | $v_{ab}$ | $D$ | $\psi$ | $H_1$ | $\frac{\omega}{2\pi}$ |
|---|---|---|---|---|---|---|---|
| $(\mathrm{cm}^{-1})$ | $(\mathrm{cm}^{-1})$ | $(\mathrm{cm}^{-1})$ | $(\mathrm{cm}^2)$ | $(\mathrm{cm}^2\mathrm{s}^{-1})$ | $(\mathrm{s}^{-1})$ | gauss | GHz |
| $-0.00703$ | 0.0241 | $5.3 \times 10^{-8}$ | $28.1 \times 10^{-16}$ | $4 \times 10^{-4}$ | $7 \times 10^{11}$ | 4.5 | 9.4 |

detected optically enabled us to observe a reduction in the fluorescence signal and two principal lines for each magnetic field direction.

The ODMR experiments carried out on the tetracene crystal gave us, the variation of fluorescence under the effect of a microwave power, whereas the PDMR experiments gave us the total variation of the photocurrent resulting from the different mechanisms.

In Figure 7 we have represented the digital simulation of the modulation by a microwave power of the triplet-triplet interaction rate constant for various orientations of the magnetic field in the *ab* plane. In the same figure we have reported the modulation of the triplet-doublet interaction rate constant. One can distinguish two symmetrical ODMR lines starting from the central field $H_0 = 3390$ gauss of the PDMR central line.

One can notice that, for each direction of the magnetic field, the positions of two ODMR lines coincide with the two symmetrical lines of the PDMR spectrum

According to Figures 6, 7 we can notice that the central line of the experimental spectra (Fig. 4a and Fig. 4b) results only from the modulation of the photocurrent coming from the triplet-doublet interaction.

It is thus possible to evaluate the different physical parameters $(\beta, \lambda, \tau)$ characterizing the triplet-doublet interaction starting from the expressions of the full-width at half maximum of the PDMR line and by using kinematics theory.

We have used the expressions of the relative variation of the photoconductivity given by relations (59–62) to reproduce the experimental PDMR spectrum of the tetracene.

We start by trying to find the best fit to the experimental PDMR line with the central line of the theoretical spectrum of the triplet-doublet interaction rate constant modulation.

Figure 8a shows the best agreement obtained *via* relations (59–62) for the experimental PDMR spectrum which we carried out on a crystal of tetracene. The shape of the line is reproduced perfectly with the kinematics parameters reported in Table 3. From the fit one gets:

$$\beta = 6.3 \pm 0.1 \times 10^7 \ \mathrm{s}^{-1}$$
$$\lambda = 7.5 \times 10^{12} \ \mathrm{s}^{-1}.$$

These parameters reproduce also acceptably the static lines [19] obtained in the presence of a static field only.

Since the total modulation of the photocurrent that one observes comes from the contribution of fluorescence $(\Delta F/F)$ with a weight of value "**a**" and of the interaction triplet-doublet with a weight of value "**b**" according to the expression (21). A graphic treatment enables us to determine the contributions of the modulation of the constant of interaction triplet-triplet and the constant of

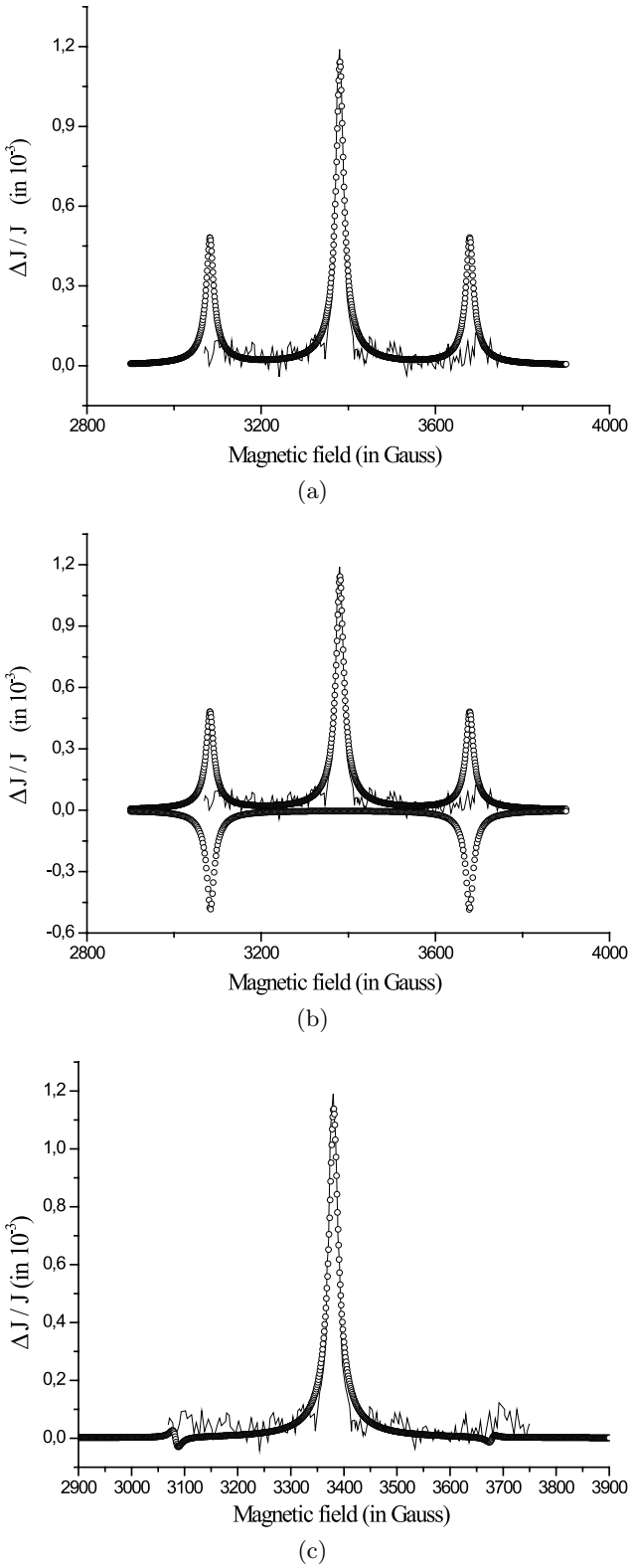


**Fig. 8.** The best fit obtained by the kinematic theory. (a) fitting of the central line width triplet-doublet interaction rate constant ($\Delta R/R$). (b) fitting of the PDMR spectrum width triplet-doublet interaction rate constant ($\Delta R/R$) and triplet-triplet interaction rate constant $\left(\Delta\gamma_s^{'}/\gamma_s^{'}\right)$. (c) the best fit obtained for the PDMR spectrum *via* the weights $a \simeq 0.2$ and $b \simeq 0.6$.

interaction triplet-doublet which are about:

$$a \simeq 0.2$$
$$b \simeq 0.6.$$

Thus, the rate constant of the detrapping by the singlet and the triplet excitons have the following value: $\delta = 0.25$.

In Figures 8b and 8c we have represented the best agreement between the experimental and theoretical PDMR lines *via* relations (21) and (59–62).

The full-width at half maximum $\Delta H$ of PDMR line is given by the relation [27]:

$$\Delta H = 2r\beta, \tag{64}$$

$\Delta H = 12,5$ gauss for a direction of the field $\varphi = 20°$ with the crystalline axis $\vec{a}$ corresponding to the value $\beta = 6.4 \times 10^7\ \mathrm{s}^{-1}$. The lifetime of the correlated triplet-doublet pair is:

$$\tau = \frac{1}{2\beta} = 7 \times 10^{-9}\mathrm{s}.$$

The triplet-doublet pair lifetime within the framework of this model is slightly higher than that obtained for the triplet-triplet pair ($2.1 \times 10^{-9}$) [26].

## 6 Conclusion

After the study of the photoconductivity modulation by an external magnetic field in crystalline tetracene [14], we have studied in this paper the effect of a microwave field on this photoconductivity.

The comparison of the observed effects on the fluorescence and the photocurrent enabled us to obtain for the first time the contribution of the modulation by a microwave field of the triplet-doublet interaction rate constant (detrapping photocurrent) and the triplet-triplet interaction rate constant (fluorescence).

The interpretation of the experimental results allows us to show that the process of detrapping carriers trapped by the triplets is more important than that trapped by the singlets, and that the modulation of the photocurrent by the microwave field results at the same time from the modulation of the singlet exciton density and the triplet-doublet interaction rate constant.

The application of the kinematics theory enabled us to suitably reproduce the observed effects and to reach the various physical parameters characterizing the triplet-doublet interaction $(\beta, \lambda, \tau)$.

The experimental study that we carried out permitted us to obtain the signature of the triplet-doublet pair and the triplet-triplet pair on the photoconductivity in the form of one central line only.

The kinematic theory reproduces nearly perfectly the shape of the PDMR line in the contrast to the kinetic theory [12] which always gives a broad line of Lorentzian form as in the ODMR experiments [26]. Furthermore, the kinetics parameters cannot be appropriately applied at the same time for the static and dynamic experiments [26].

## References


1. D.J. Carswell, L.E. Lyons, J. Chem. Soc., 1734 (1955)
2. P. Delannoy, thesis, Paris (1977)
3. Vaubel, G. and Baessler, H., Phys. Lett. A **27**, 328 (1968)
4. A. Many, J. Levison, I. Teucher, Mol. Cryst. **5**, 273 (1969)
5. C.E. Swenberg, W.T. Stacy, Chem. Phys. Lett. **2**, 327 (1968)
6. N.E. Geacintov, M. Pope, S.J. Fox, Phys. Chem. Solids **31**, 1375 (1970)
7. N.E. Geacintov, F. Pope Vogel, Phys. Rev. Lett. **22**, 593 (1969)
8. R.P. Groff, P. Avakian, R.E. Merrifield, Phys. Rev. B **1**, 815 (1970)
9. H. Bouchriha, V. Ern, J.L. Fave, C. Guthmann, M. Schott, J. Phys. **39**, 257 (1978)
10. H. Bouchriha, V. Ern, J.L. Fave, C. Guthmann, M. Schott, Phys. Rev. B **18**, 525 (1978)
11. R.C. Johnson, R.E. Merrifield, Phys. Rev. B **1**, 896 (1970)
12. A. Suna, Phys. Rev. B **1**, 1716 (1970)
13. Y. Tomkwicz, R.P. Groff, P. Avakian, J. Chem. Phys. **54**, 4504 (1971)
14. F. Henia, thesis Tunis (1987)
15. H. Bouchriha, thesis, Paris (1978)
16. H. Bouchriha, J.L. Monge, V. Ern, S. Romdhane, A. Ben Fredj, J. Phys. I France **3**, 203 (1993)
17. P. Delannoy, M. Schott, Phys. Lett. A **30**, 357 (1969)
18. F. Henia, J.L. Monge, P. Delannoy, H. Bouchriha, J. Phys. France **47**, 649 (1986)
19. F. Henia, J.L. Monge, H. Bouchriha, J. Phys. France **48**, 2097 (1986)
20. P. Avakian, E. Abramson, R.G. Kepler, J.C. Caris, J. Chem. Phys. **39**, 1127 (1963)
21. R.E. Merrifield, P. Avakian, R.P. Groff, Chem. Phys. Lett. **3**, 155 (1969)
22. M. Mejatty, J.L. Monge, V. Ern, H. Bouchriha, Phys. Rev. B **36**, 2735 (1987)
23. M. Mejatty, J.L. Monge, V. Ern, H. Bouchriha, J. Phys. France **47**, 659 (1986)
24. P. Avakian, A. Suna, Matter. Res. Bull. **6**, 891 (1971)
25. V. Ern, in *Energy Transfer Processes in Condensed Matter*, edited by B. DiBartolo (Plenum, New York, 1984), pp. 371–451
26. T. Barhoumi, thesis, Tunis (2002)
27. M. Mejatty, J.L. Monge, V. Ern, H. Bouchriha, Phys. Rev. B **43**, 2558 (1991)